Power System Technology
ISSN:1000-3673

Received: 06-05-2024 Revised: 15-06-2024 Accepted: 28-07-2024

Targeted Electroless Copper Plating on Ink-Jet Printed Textiles with a Copper-Silver Nanoparticles Catalyst

Bilal Muslim[1], Hafiz Muneeb Shahid[1], Raza Rabbani[2], Farah Qayyum[2]

1. School of Engineering & Technology, National Textile University, Faisalabad, 37610, Pakistan

2. Institute of Chemistry, Khwaja Fareed University of Engineering and Information Technology (KFUEIT) R Y K, Pakistan

ABSTRACT

Electroless copper plating is a viable method that can be used to deposit Copper selectively to the textile substrates to produce sensors, high-reliability e-textiles, and wearable electronics for various applications that include health monitors, sportswear, military, and others that are demanding high performance in unique value chain markets. Any textiles that are planned to be coated with the polymer layer must first be printed with a catalyst. In this work, polyester fabrics were ink-jet printed with a functionalized copper-silver nanoparticles catalyst in different amounts and dispositions before being electroless copper plated. UV/Vis spectroscopy and Transmission Electron Microscopy (TEM) were used to characterize the catalyst. Scanning electron microscopy was used to assess the shape and plating coverage of the fibers as well as the copper mass gain, appearance, and electrical resistance of the electroless copper coatings. A Launder Ometer and a rigidity tester were also used to assess the textiles' color fastness and stiffness, respectively. Based on the textile's structure, the results showed that the printing design, printing direction, and total number of printing cycles of the catalyst must be carefully tuned to give a metalized pattern with the appropriate conductivity, stiffness, and washing durability for e-textiles. A full copper coating that is highly conductive and has nearly equal and acceptable stiffness on both sides of the fabric can be taken into consideration as helpful markers to assess the process's appropriateness.

Keywords: Ink-jet printing, Textile, Electroless Copper Plating, Catalyst, Copper-Silver Nanoparticles

INTRODUCTION

The integration of textile technology with electronics for forming stimuli-responsive matrices is a rather current trend that has propelled great progress in the growth of smart textiles (Wills et al., 2018). These innovations are potentially applicable in health, sporting activities, military, and consumer electronics industries. Integrated conductive pathways throughout the fabric are essential to these smart textiles' operation (Xie et al., 2023). Previous approaches to the

Power System Technology
ISSN:1000-3673
Received: 06-05-2024 Revised: 15-06-2024 Accepted: 28-07-2024

formation of such pathways, however, are associated with rather labor-intensive operations that may negatively impact the overall versatility, feel, and looks of these fabrics (Tong and Tong, 2022). This study aims to investigate the integration of the necessary conductive pathways directly into textiles using an electroless copper plating procedure where a catalyst based on inkjet-printed copper-silver nanoparticles has been used for this purpose.

Electroless plating is one of the chemical reduction processes to form a metallic layer onto the substrate without any electrical current and it is felt to be a good method of depositing a metallic layer onto the fabric to make it conductive (Xiao et al., 2022). There are several potential benefits associated with this method, including better distribution of the metal, as well as the efficient coating of different structures of the given geometry, and the lack of need for electrical contacts during the process of plating (Thakur and Murthy, 2021). Nonetheless, the traditional electroless plating techniques sometimes prove relatively imprecise in placing the metallic layers on the required zones of the textile substratum (Mondin, 2014). This limitation may cause a waste of material, and result in undesired surface coverage that does not enhance the basic purpose and aesthetics of the smart textile (Feng and Zhu, 2019).

To overcome such challenges, new applications of ink-jet printing and electroless plating technology are becoming sophisticated solutions (Rayhan et al., 2023). Ink-jet printing, which is considered a more accurate and flexible technique, allows for the deposition of functional inks at defined locations (Mohsen et al., 2024). Thus, using this technology one can create a selective deposition of a catalyst on the textile substrates, and due to this have more precise control over further electroless plating (Zhu et al., 2018). The catalyst part consists of copper-silver nanoparticles which provide effective seeding for proper and more electroless copper deposition along with the proper growth of the subsequent conformal structures with specific requirements for accessional conjugate conductivity (Pandey et al., 2021).

The advantages of employing copper-silver nanoparticles as a catalyst can be understood from the properties they provide (李万里, 2018). Among all metals, copper is widely used for the fabrication of conductive paths due to its excellent electrical conductivity. However, copper nanoparticles are easily oxidized copper nanoparticles which is not desirable especially when used for conductor purposes similar to the case with silver nanoparticles. Silver, in turn, describes relatively good oxidation resistance and improves the stability of the catalyst. When these two metals are combined at the nanoscale, each metal contributes distinct properties that create synergistic effects for both the efficacy and longevity of the catalyst (Cherrington and Liang, 2016).

The objective of this work is to explore comprehensively the factors that affect the formation of the desired electroless copper pattern on ink-jet printed fabric broads. This allows for arbitrary and reproducible patterns of the catalyst to be applied to a variety of textile materials

Power System Technology
ISSN:1000-3673
Received: 06-05-2024 Revised: 15-06-2024 Accepted: 28-07-2024

through appropriate optimization of the ink formulation and the printing process. Future trials of electroless plating will involve the enhancement of chemical solutions and plating parameters to achieve the desired and uniform particles of copper on the textile fabric coupled with good adhesion.

METHODOLOGY

The textile substrate used in this study was Polyester Crepe de Chine White which was obtained from Whaleys Ltd., Bradford, UK. This fabric has a plain weave, 0.32 mm of thickness, and 120 g/m^2 of mass per unit area. The thread densities attained were 69 ends per centimeter "(EPC) and 30 picks per centimeter (PPC). Reagents for the synthesis of copper-silver nanoparticles (Cu–Ag NP) catalysts were purchased from Sigma-Aldrich, Germany. These included copper (II) acetate monohydrate (98%), poly(acrylic acid, sodium salt) solution (average Mw ~8000, 45 wt.% in H_2O), hydrazine (64–65%, reagent grade, 98%), and silver nitrate (ACS reagent, ≥99.0%). Additional reagents such as ammonia solution (30% ROTIPURAN®), sodium hydroxide (≥98%, p.a., ISO, in pellets), and ethanol (≥96%, denatured) were procured from Carl Roth (Karlsruhe, Germany). Circuposit Conditioner 3323A used to pre-treat the textiles and Circuposit 3350-1 used for the electroless copper electrolyte" used in this project were provided by A-Gas Electronic Materials.

Equipment

A thermal ink-jet BREVA printer of small format with the printing area of the printer being 15 cm x 15 cm was used to print the catalyst. Standard empty HP45 cartridges were loaded with the Cu–Ag NP catalyst, and placed into the printer. The voltage and pulse width of the ink cartridge were tuned to 13.3 V and 2.7 µs, respectively.

Synthesis of Cu–Ag NP Catalyst

The synthesis of the Cu–Ag NP catalyst involved three main steps: (i) synthesis of Cu NPs, (ii) modification of Cu NPs with polyacrylic acid (PAA), and (iii) formation of an Ag shell on the stabilized Cu NPs (Azar et al., 2020).

1. Synthesis of Cu NPs: An aqueous solution of copper-ammonia complex and copper (II) hydroxide was used as the copper source, which was then reduced by hydrazine.

2. Modification with PAA: PAA was added to functionalize the Cu NPs, followed by the addition of ethanol. The mixture was stirred for 1 hour, and the particles were subsequently separated, washed, and re-dispersed in water using an ultrasonic bath. The concentration ratio of Cu NPs to PAA was approximately 1:1.3–1:1.5.

3. Formation of Ag Shell: A 0.1 M $AgNO_3$ solution in 2.5 M NH_4OH was gradually added to the Cu NP-PAA colloid, leading to the deposition of Ag onto the Cu NP surface. This caused

Power System Technology
ISSN:1000-3673
Received: 06-05-2024 Revised: 15-06-2024 Accepted: 28-07-2024

a color change from red wine to deep black. The Cu–Ag NP colloid with 5 at.% Ag concentration was selected for this study.

Printing of Cu–Ag NP Catalyst and Electroless Plating

The pieces of the textile samples were taken in the form of 8 cm x 4 cm each as per the warp and weft directions. These samples were subjected to Circuposit Conditioner 3323A pre-treatment step following the manufacturer's specifications; at 50°C for 5 min, washed and dried at 45°C for night. These were arranged on the printer stage and the Cu–Ag NP catalyst was printed in certain design patterns with varying cycles selected as 2, 3, 4, and 5 with four trials each. The printed textiles were then treated with Circuposit 3350-1 electroless copper electrolyte at 46°C for half an hour, subsequently washed with running water for half an hour, and then left for drying for a whole night.

Characterization of the Samples

Characterization of Cu–Ag NP Catalyst

The suitable Ag concentration for the shielding of Cu NPs was determined using UV/Vis spectroscopy on Hitachi U-2001 UV/Vis spectrometer. The morphological features of the Cu–Ag NP catalyst and to determine the size and distribution of the nanoparticles were characterized by transmission electron microscopy (TEM) using an FEI Talos F200X.

Characterization of Electroless Copper Coatings

The increase of mass in copper of the textiles was determined by weighting each of the samples after cutting into pieces (8 cm x 4 cm) and after electroless copper plating and drying at 100°C for one day. The morphology of the copper coatings and the degree of fiber coverage were characterized using a ZEISS GEMINI 500 VP SEM. To determine the electrical resistance of the metalized patterns, a multimeter was used to obtain readings from the outermost edges of both dumbbell patterns.

Textile Characterizations

ATM-D1388-96 was employed in using a Shirley stiffness tester to determine the stiffness of the metalized textiles (Jahan, 2017). Washing fastness tests were conducted according to ISO 105-C06 (A1S):2010. Cycles of washing were performed on the samples while resistance measurements were done on them to determine their performance and life span.

This methodology combines the control of catalyst deposition on the textile surface with the rest of the parameters in the electroless plating process in a bid to form highly conductive and durable, flexible textile substrates for applications in smart textiles.

Power System Technology
ISSN:1000-3673
Received: 06-05-2024 Revised: 15-06-2024 Accepted: 28-07-2024

RESULTS AND DISCUSSION

UV/Vis Spectroscopy Characterization

When Ag ions came into contact with the Cu NPs in a solution during the manufacture of Cu–Ag NP colloids using the methodology used in this study, Ag became embedded in Cu NPs as a result of a spontaneous galvanic replacement. Ag ions were then reduced into atoms and placed on the surface of the Cu NPs, whilst Cu atoms were oxidized into ions and dispersed into the solution. To guarantee the collision and deposition of the Ag atoms on the Cu NPs, the Ag precursor was injected into the Cu NP colloid at a suitably slow rate to establish a low Ag ion concentration surrounding the Cu NPs. Cu_{core}-Ag_{shell} NPs were therefore anticipated to be the primary output of our synthesis process.

UV/Vis spectroscopy was performed on the diluted Cu–Ag NP colloids to ascertain the proper Ag concentration to shield Cu NPs from oxidation and to comprehend the structure of the synthesized Cu–Ag NPs. The optical spectra of the synthesized Cu–Ag NP colloids at various Ag concentrations are displayed in **Figure 1a**. Only the copper plasmon peak at 565 nm was visible in the surface plasmon spectra of the pure Cu NPs (black line). The absorbance corresponding to silver (at 443 nm) developed with the addition of Ag to the Cu NP colloid (red line). When contrasted to the unadulterated Ag NPs peak (at about 405 nm) (Byeon and Kim, 2012), the observed absorption peak displayed a redshift. The absorption rose along with the Ag content in the colloid, and the absorption peak moved further into the red area. Cu–Ag bimetallic NPs are the predominant products, as indicated by the redshift and broadening of the surface plasmon resonance (SPR) band, according to Byeon et al (Byeon and Kim, 2012). However, the 565 nm copper plasmon peak vanished with greater Ag concentrations. Binary metal or alloy NPs typically exhibit two separate surface plasmons in their UV/Vis spectra (Karim et al., 2017). Conversely, in the scenario of core-shell NPs, just one single peak at a wavelength near the shell metal's SPR peak may be seen because of the development of shell metal on the core metal's surface. Cu_{core}-Ag_{shell} NPs were therefore probably the majority in the produced Cu–Ag NP colloids with a suitable Ag concentration. Other studies have reported similar outcomes (Sakthisabarimoorthi et al., 2017, Kumar et al., 2021, Mallick et al., 2015). Moreover, symmetric peaks and suitably narrow surface plasmons suggested that the majority of the particles were spherical in shape (Pajor-Świerzy et al., 2017).

Power System Technology
ISSN:1000-3673
Received: 06-05-2024 Revised: 15-06-2024 Accepted: 28-07-2024

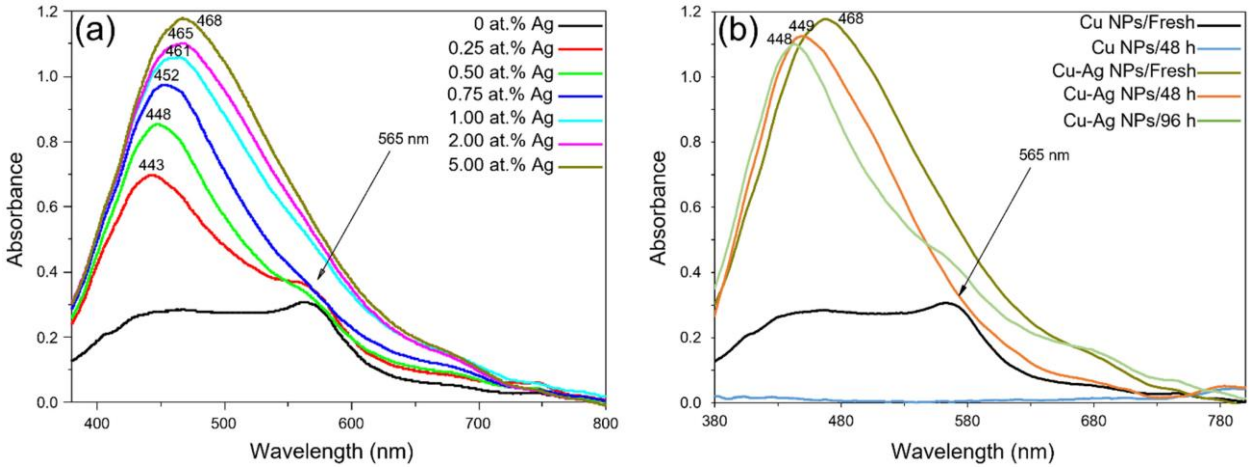

(Pellarin et al., 2015)

Figure 1: (A) Optical spectra of Cu–Ag NP colloids (diluted) at different silver concentrations (B) optical spectra of Cu NP and Cu–Ag NP (~5 at.% Ag) colloids (diluted) at different times after their synthesis.

The creation of the Ag shell on Cu NPs to shield them from air oxidation was one of the goals of this effort. As a result, up to 96 hours after synthesis, the oxidation process of the created Cu–Ag NPs was examined and contrasted with the behavior of pure Cu NPs. The optical spectra of the produced pure Cu NPs and Cu–Ag NPs (containing approximately 5 at.% Ag) across various periods are displayed in **Figure 1b**. Within 48 hours of their manufacture, pure Cu NPs were seen to be oxidized and dissolved (red line). Cu–Ag NPs, on the other hand, were more stable because the surface plasmon peak (light blue line) in the optical spectrum corresponding to the Ag shell was still visible 96 hours later (Pellarin et al., 2015). The segregation of Cu and Ag in particles and oxidation of the Cu core may be connected to the blue shift of the silver plasmon peak with time and the emergence of a shoulder in the copper plasmon region (Figure 2b). As a result, Cu–Ag NP colloid containing around 5 at.% Ag was utilized for subsequent characterizations and subsequently as a catalyst for electroless copper plating textiles.

TEM Characterization

The structure of the synthesized Cu-Ag NP catalyst, as well as the dimensions and placement of the Cu and Ag NPs, were examined using TEM (Figure 2). Particles of various sizes were present in the Cu–Ag NP colloid, as shown in Figure 2 a,b. These included smaller NPs measuring 10–20 nm and bigger NPs or particle aggregates measuring 60–70 nm. Large particles were easily apparent in the Cu distribution mapping image (Figure 2c), whereas smaller particles showed weak contrast because of their lower mass or partially obscured signal by Ag. On the other hand, Figure 2d's Ag distribution mapping graphic was more intricate. The

Power System Technology
ISSN:1000-3673
Received: 06-05-2024 Revised: 15-06-2024 Accepted: 28-07-2024

Ag's size and shape were largely comparable to the Cu NPs', with considerable contrast on smaller particles and barely perceptible on larger ones. This discovery may be explained by the smaller Cu NPs' increased surface-to-volume ratio, which promotes Ag ion collisions and the nucleation of Ag atoms to form the shell. This results in a thinner Ag shell on big Cu NPs, which may be difficult to see in TEM, but whose presence was confirmed by UV/Vis spectroscopic investigation. Cu NP, measuring around 70 nm in size, is seen in Figure 2e with an Ag shell that is roughly 1-3 nm thick. As a result, even at an Ag shell thickness equal, the Ag/Cu ratio sharply dropped as Cu NP size increased. The higher contrast of Ag on the smaller nanoparticles and the higher contrast of Cu on the larger nanoparticles are both seen in Figure 2f.

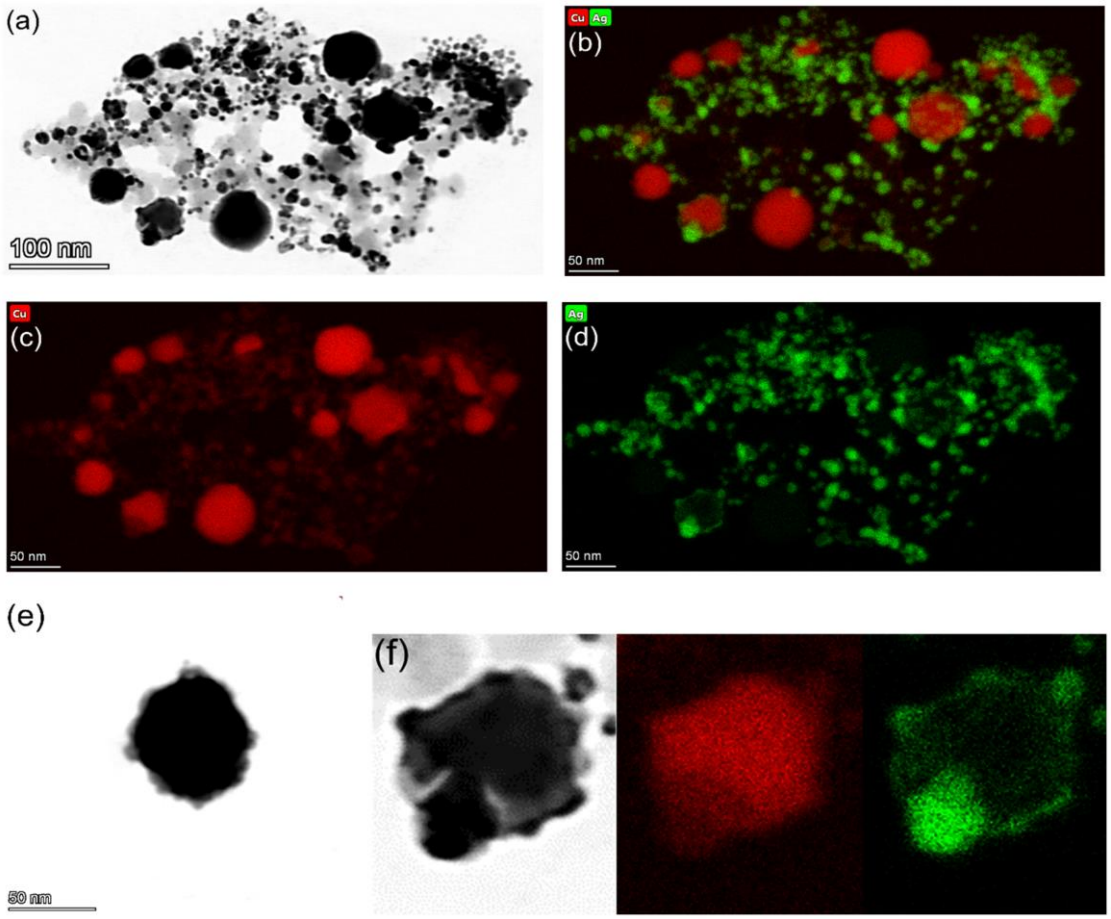

Figure 2: (a) TEM micrograph of the Cu–Ag NP catalyst; X-ray elemental mapping images of (b) Cu & Ag; (c) Cu; and (d) Ag; (e) TEM image of a single Cu_{core}–Ag_{shell} NP; and (f) partial sections of TEM image, and Cu and Ag X-ray elemental mapping images showing the higher contrast of Ag on the smaller particles and higher contrast of Cu on the larger particles.

Power System Technology
ISSN:1000-3673
Received: 06-05-2024 Revised: 15-06-2024 Accepted: 28-07-2024

For metal nanoparticles (NPs), the placement of the plasmon bands of absorption is determined by their size and form; however, for core-shell NPs, the thickness of the shell also plays a role (Paszkiewicz et al., 2016). The Ag plasmon peaks that were found, which were substantially larger than those in Figure 2d, and fell between 440 and 470 nm, corresponded to pure Ag NPs that were 60 to 80 nm in size. Consequently, rather than being caused by the existence of pure Ag NPs, the detected Ag plasmon peaks were most likely connected to the core-shell structure (Singh et al., 2013).

Characterisation of Electroless Copper Coatings

The amount of copper that is gained and the way the textiles look after electroless plating are crucial markers for comparing how well catalysts—in this case, various catalyst printing conditions—allow electroless plating. The purpose of these investigations in the context of our study was to ascertain the impact of printing direction and catalyst NP loading (various counts of printing cycles) on the electroless copper coatings that were deposited. The electroless copper mass gain of the specimens, which were printed ink-jet using the Cu–Ag NP catalyst at varying printing cycle counts and orientations, is displayed in Figure 4. The copper mass gain rose as predicted as the quantity of catalyst printing cycles increased, however, the rate peaked at higher printing cycles. More catalytic Cu and Ag NPs were added to the surface during each printing cycle, significantly facilitating electroless copper plating and increasing copper mass gain.

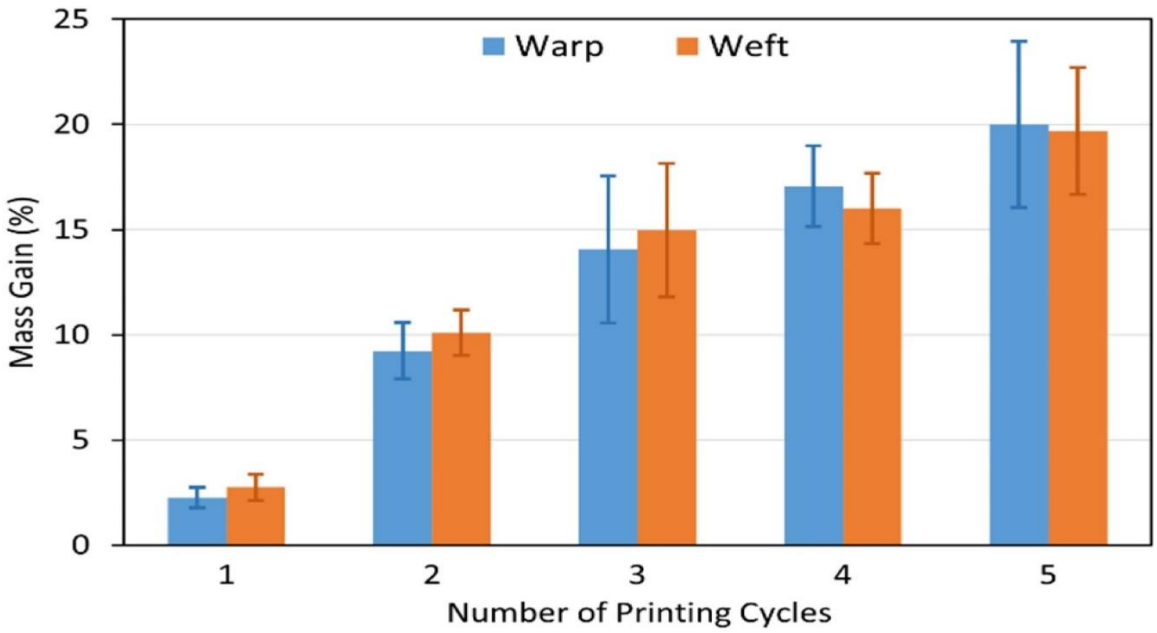

Figure 3: Electroless copper mass gain of textile samples printed with the Cu–Ag NP catalyst at different numbers of cycles and directions.

Power System Technology
ISSN:1000-3673
Received: 06-05-2024 Revised: 15-06-2024 Accepted: 28-07-2024

When it came to the impact of printing direction, following electroless plating, the copper mass gain of the specimens printed with a catalyst at the same amount of cycles in various orientations was similar (Figure 3). This outcome clearly indicates that the electroless copper mass gain is mostly unaffected by the printing direction of the catalyst. The spreading behavior of the electroless copper coatings and their reliance on the printing direction, however, was a highly intriguing discovery made during the visual inspection. As the amount of printing cycles grew, spreading became more pronounced in both printing directions. Conversely, on the material printed in the weft direction, spreading was often more pronounced at the identical number of printing cycles. The metallized patterns that were printed in the warp direction with the catalyst primarily had sharper edges and more closely matched original designs in terms of size. Hajipour et al. found similar outcomes when they looked into how the polyester fabric's weave structure affected the caliber of ink-jet printing employing water-based ink. Ink was dispersed in the weft direction for patterns printed in the warp direction; the amount of ink spread was regulated by the density of the weft threads floating on top of the warp yarns. Diffusion of ink occurred in the warp direction, however, when patterns were printed in the weft direction. They came to the conclusion that the ink dispersion was controlled by the density of the warp strands floating on top of the weft yarns. It follows that this kind of ink spreading, which is parallel to the printing direction, happens in both situations. On the other hand, the warp yarn density (69 vs. 31/cm) in the polyester textile employed in this investigation was more than double that of the weft yarn density. For patterns printed in the weft direction, the ink therefore spread more strongly perpendicular to the printing direction. The explanation was most likely that there was insufficient catalytic ink distributing in the direction of weft for the designs printed in the warp direction, which prevented the electroless copper plating from starting across the spread area.

Electrical Resistance Measurements

Using a multimeter, the electric resistance of the electroless copper coating on the polyester textiles printed with the Cu–Ag NP catalyst at various intervals and orientations was determined. Figure 4 illustrates the outcomes. The thickness, level of coverage, and depth of the electroless copper coatings determine the conductivity of the metallized patterns. Figure 4 illustrates how resistance dropped as the number of printing cycles grew in both printing orientations. The higher electroless copper mass gain for the greater number of catalyst printing cycles across both printing directions was consistent with this outcome. However, during the same number of printing cycles, the metallized pattern printed in the weft direction with the catalyst had more resistance than the design printed in the warp direction.

Power System Technology
ISSN:1000-3673
Received: 06-05-2024 Revised: 15-06-2024 Accepted: 28-07-2024

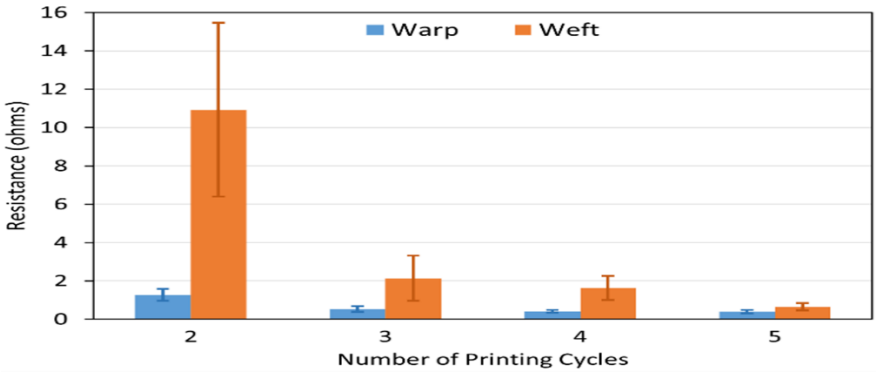

Figure 4: Electrical resistance of the metallised patterns printed with the Cu–Ag NP catalyst at different numbers of cycles and directions.

Fabric Stiffness Test

To be used as wearable electronics for a variety of applications, selectively metalized textiles must be comfortable to wear as well as multifunctional. Among the most crucial aspects of the textiles is their stiffness, which affects their adaptability, drape, and management properties. An indicator of the textiles' stiffness is their bending resistance, which was measured using a stiffness tester on the bending lengths of the metalized textiles printed with the Cu–Ag NP catalyst at various printing cycles and directions. Figure 5 shows the results, which were compared to those for a control sample. As can be observed, the control sample featured identical bending lengths across the fabric's face and back, whereas the weft-way sample had a shorter bending length than the warp-way sample. As previously indicated (Lolaki and Shanbeh, 2020), the textile's warp way (finer yarn with 69 EPC) and weft method (coarser yarns with 30 PPC) differed, which affected the cover factor. One of the primary factors influencing the fabrics' capacity to bend is the cover factor. The weft, warp, and total fabric cover factor have the greatest effects on how stiff the textiles are (Nawab, 2017).

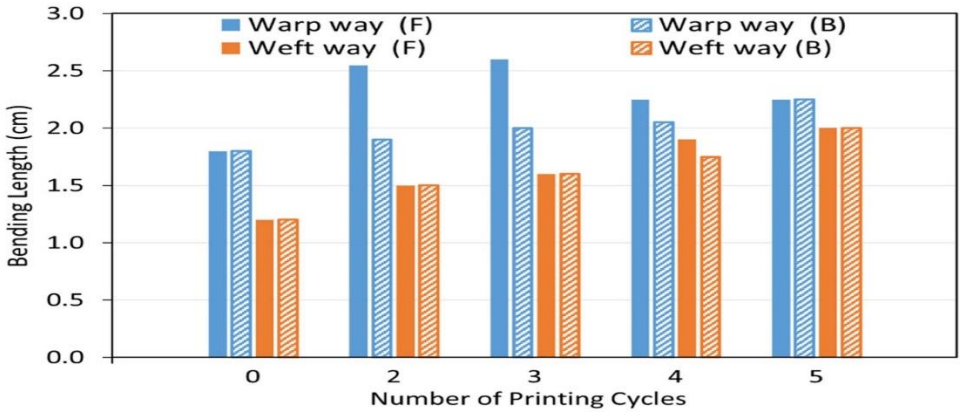

Figure 5: Bending lengths of the face (F) and back (B) side of the metalized textiles printed with the Cu–Ag NP catalyst at different numbers of cycles and directions.

Power System Technology
ISSN:1000-3673
Received: 06-05-2024 Revised: 15-06-2024 Accepted: 28-07-2024

Following each washing cycle, the color shift on the cleaned specimens and the color staining on the white multifibre textiles from the metalized samples were visually evaluated using the ISO standard Grey Scales. **Table 1** presents the results. It was found that there was no discernible variation in the color staining of any of the metalized samples, regardless of the number of cycles, direction, or washing sessions of the catalyst printing. The color staining grade was rated as Good with a score of 4/5. This suggested that the white multifibre fabrics had only a minor discoloration, which was acceptable (Danilova et al., 2021). The existence of metallic copper particles on the metalized samples was most likely the cause of this color shift. These particles, however, did not stick to the white multifiber textiles' surface (Hajipour and Shams Nateri, 2019). Conversely, the metalized samples at the higher number of washing cycles exhibited the lowest grade of color alteration (shade change) at three. This could be because of how the detergent affects the water, mechanical force, and particles of copper during washing sessions.

Table 1. Colour fastness of the metallised textiles printed with the Cu–Ag NP catalyst at different numbers of printing cycles and directions.

No. of Printing Cycles/Fastness	Washing Cycles									
	Warp Way Sample					Weft Way Sample				
	1	2	3	4	5	1	2	3	4	5
2/Colour change	4/5	4	3			4/5	3	3		
2/Colour staining	4/5	4/5	4/5			4/5	4/5	4/5		
3/Colour change	4/5	4/5	4			4/5	4	4	3/4	
3/Colour staining	4/5	4/5	4/5			4/5	4/5	4/5	4/5	4/5
4/Colour change	4/5	4	4	3/4		4/5	4	4	3/4	
4/Colour staining	4/5	4/5	4/5	4/5		4/5	4/5	4/5	4/5	

Power System Technology
ISSN:1000-3673
Received: 06-05-2024 Revised: 15-06-2024 Accepted: 28-07-2024

5/Colour change	4/5	4	4	4	4	4/5	4	4	3/4	3/4
5/Colour staining	4/5	4/5	4/5	4/5	4/5	4/5	4/5	4/5	4/5	4/5

CONCLUSIONS

The functionalized Cu–Ag NP catalyst was effectively synthesized in this study and employed as an ink-jet printing ink to selectively catalyze the polyester textiles. Copper is proved to be protected from oxidation by the synthesized catalyst's core-shell structure. Various printing parameters, such as the quantity of printing cycles and printing directions, were used during the ink-jet printing of the catalytic ink to observe how they affected the final characteristics of the metalized textiles. In both printing directions, the electroless copper mass gain was improved by increasing the number of printing cycles. The fabrics printed in the weft direction, particularly at lower printing cycle counts, had poorer conductivities than those printed with the catalyst, although having identical electroless copper mass gains after a similar number of printing cycles. This was most likely due to the nature of the textile, which caused an overall spread of more ink on fabrics printed in the weft direction when using the catalyst. Subsequently, it is found that the inclusion of the composition of the textile and other aspects of printing characteristics that include, printing design, direction of printing, and the number of printing circles substantially alleviate the problem of ink spreading.

The metalized samples had less stiffness on the weft path at the equivalent quantity of printing cycles because the weft cover factor was lower than the warp cover factor. Irrespective of the number of printing cycles, the weft way stiffness was identical on the face and back side of the metalized samples due to the more extensive absorption of catalytic ink by fibers caused by a lower weft cover factor. Conversely, for the warp-way metalized samples, stiffness at the lower number of printing cycles varied significantly between the metalized samples' face and back. At greater printing cycles, though, it started to resemble each other.

The reverse of metallized samples printed by the catalyst at every cycle exhibited fully electroless copper coatings that were highly conductive, regardless of printing orientation. Following each washing cycle, the conductivity of the metallized samples decreased for any number of printing cycles and directions. When the amount of washing cycles increased, the decline grew more significant, even if it was initially just moderate. For every sample that was metallized, the color staining grade was deemed Good (grade 4/5), and the lowest grade of color change only happened when there were more washing cycles.

Power System Technology
ISSN:1000-3673
Received: 06-05-2024 Revised: 15-06-2024 Accepted: 28-07-2024

The study's findings, for the first time, highlight the significance of comprehending the structure of textiles, including the density, thickness, and cover factor of the yarns in the warp and weft directions, and how these factors affect the metallized textiles' conductivity, stiffness, and laundering durability. As a result, printing parameters for each unique textile should be adjusted to deposit the catalyst in a way that can produce a metallized pattern with the required qualities to be used as e-textiles.

REFERENCES

1. AZAR, G. T. P., FOX, D., FEDUTIK, Y., KRISHNAN, L. & COBLEY, A. J. 2020. Functionalised copper nanoparticle catalysts for electroless copper plating on textiles. *Surface and Coatings Technology*, 396**,** 125971.
2. BYEON, J. H. & KIM, Y.-W. 2012. Aerosol copper initiated core–shell nanoparticle synthesis and micropatterning. *New Journal of Chemistry*, 36**,** 2184-2187.
3. CHERRINGTON, R. & LIANG, J. 2016. Materials and deposition processes for multifunctionality. *Design and Manufacture of Plastic Components for Multifunctionality: Structural Composites, Injection Molding, and 3D Printing***,** 19-21.
4. DANILOVA, S., GRAVES, J. E., SORT, J., PELLICER, E., CAVE, G. W. & COBLEY, A. 2021. Electroless copper plating obtained by Selective Metallisation using a Magnetic Field (SMMF). *Electrochimica Acta*, 389**,** 138763.
5. FENG, Y. & ZHU, J. 2019. Copper nanomaterials and assemblies for soft electronics. *Sci. China Mater*, 62**,** 1679-1708.
6. HAJIPOUR, A. & SHAMS NATERI, A. 2019. The effect of weave structure on the quality of inkjet polyester printing. *The Journal of the Textile Institute*, 110**,** 799-806.
7. JAHAN, I. 2017. Effect of fabric structure on the mechanical properties of woven fabrics. *Advance Research in Textile Engineering*, 2**,** 1018.
8. KARIM, N., AFROJ, S., TAN, S., HE, P., FERNANDO, A., CARR, C. & NOVOSELOV, K. S. 2017. Scalable production of graphene-based wearable e-textiles. *ACS nano*, 11**,** 12266-12275.
9. KUMAR, R., KAUSHIK, R., KUMAR, R., JOSE, D. A., SHARMA, P. K. & SHARMA, A. 2021. Facile synthesis of CucAgs based nanoparticles and nanocomposites as highly selective and sensitive colorimetric cyanide sensor. *Materials Chemistry and Physics*, 260**,** 124132.
10. LOLAKI, A. & SHANBEH, M. 2020. Variation of Poisson's ratio of fabrics woven with helical composite auxetic weft yarns in relation to fabric structural parameters. *Journal of Industrial Textiles*, 50**,** 149-169.
11. MALLICK, S., SANPUI, P., GHOSH, S. S., CHATTOPADHYAY, A. & PAUL, A. 2015. Synthesis, characterization and enhanced bactericidal action of a chitosan

Power System Technology
ISSN:1000-3673
Received: 06-05-2024 Revised: 15-06-2024 Accepted: 28-07-2024

supported core–shell copper–silver nanoparticle composite. *RSC Advances,* 5**,** 12268-12276.

12. MOHSEN, R. M., ABU-AYANA, Y. M. & MORSI, S. M. 2024. Fabrication of Conductive Polymeric Films with Metallic Luster by Electroless Plating of Silver, Copper, and Nickel onto Polymethyl Methacrylate Beads. *Egyptian Journal of Chemistry,* 67**,** 589-597.
13. MONDIN, G. 2014. Functionalization of particles and selective functionalization of surfaces for the electroless metal plating process.
14. NAWAB, Y. 2017. Fabric Manufacturing Calculations Process and Product. *Higher Education Commission Pakistan*.
15. PAJOR-ŚWIERZY, A., FARRAJ, Y., KAMYSHNY, A. & MAGDASSI, S. 2017. Air stable copper-silver core-shell submicron particles: Synthesis and conductive ink formulation. *Colloids and Surfaces A: Physicochemical and Engineering Aspects,* 521**,** 272-280.
16. PANDEY, M., RASHIKU, M. & BHATTACHARYA, S. 2021. Recent progress in the development of printed electronic devices. *Chemical Solution Synthesis for Materials Design and Thin Film Device Applications***,** 349-368.
17. PASZKIEWICZ, M., GOŁĄBIEWSKA, A., RAJSKI, Ł., KOWAL, E., SAJDAK, A. & ZALESKA-MEDYNSKA, A. 2016. Synthesis and characterization of monometallic (Ag, Cu) and bimetallic Ag-Cu particles for antibacterial and antifungal applications. *Journal of Nanomaterials,* 2016**,** 2187940.
18. PELLARIN, M., ISSA, I., LANGLOIS, C., LEBEAULT, M.-A., RAMADE, J., LERMÉ, J., BROYER, M. & COTTANCIN, E. 2015. Plasmon Spectroscopy and Chemical Structure of Small Bimetallic Cu (1–x) Ag x Clusters. *The Journal of Physical Chemistry C,* 119**,** 5002-5012.
19. RAYHAN, M. G. S., KHAN, M., SHOILY, M. T., RAHMAN, H., RAHMAN, M. R., AKON, M. T., HOQUE, M., KHAN, M. R., RIFAT, T. R. & TISHA, F. A. 2023. Conductive textiles for signal sensing and technical applications. *Signals,* 4**,** 1-39.
20. SAKTHISABARIMOORTHI, A., JOSE, M., MARTIN BRITTO DHAS, S. & JEROME DAS, S. 2017. Fabrication of Cu@ Ag core–shell nanoparticles for nonlinear optical applications. *Journal of Materials Science: Materials in Electronics,* 28**,** 4545-4552.
21. SINGH, A., JHA, S., SRIVASTAVA, G., SARKAR, P. & GOGOI, P. 2013. Silver nanoparticles as fluorescent probes: new approach for bioimaging. *Int. J. Sci. Technol. Res,* 2**,** 153-157.
22. THAKUR, N. & MURTHY, H. 2021. Nickel-based inks for inkjet printing: a review on latest trends. *American Journal of Materials Science,* 11**,** 20-35.

Power System Technology
ISSN:1000-3673
Received: 06-05-2024 Revised: 15-06-2024 Accepted: 28-07-2024

23. TONG, C. & TONG, C. 2022. Conductive Materials for Printed Flexible Electronics. *Advanced Materials for Printed Flexible Electronics*, 119-157.
24. WILLS, K., KRZYZAK, K., BUSH, J., ASHAYER-SOLTANI, R., GRAVES, J., HUNT, C. & COBLEY, A. 2018. Additive process for patterned metallized conductive tracks on cotton with applications in smart textiles. *The Journal of The Textile Institute*, 109, 268-277.
25. XIAO, Y., LI, Q., ZHANG, C., ZHANG, W., YUN, W. & YANG, L. 2022. Fabrication of silver electrical circuits on textile substrates by reactive inkjet printing. *IEEE Sensors Journal*, 22, 11056-11064.
26. XIE, J.-Q., TIAN, J., MAO, L., CAO, H., ZHOU, B., SHI, L., HOU, S., JI, Y. & FU, X.-Z. 2023. A facile and universally applicable additive strategy for fabrication of high-quality copper patterns based on a homogeneous Ag catalyst ink. *Chemical Engineering Journal*, 477, 147115.
27. ZHU, C., LI, Y. & LIU, X. 2018. Polymer interface molecular engineering for E-textiles. *Polymers*, 10, 573.
28. 李万里. 2018. *Development of low temperature curable Cu inks.* 博士論文.